Polyhedron 31 (2012) 558–564

Contents lists available at SciVerse ScienceDirect

Polyhedron

journal homepage: www.elsevier.com/locate/poly

Three-dimensional triazenido layers attained through classical and non-classical hydrogen interactions and its coordination to palladium under prolific occurrence of bifurcated hydrogen bonding

Davi Fernando Back, Manfredo Hörner *, Fernanda Broch, Gelson Manzoni de Oliveira *

Departamento de Química, Universidade Federal de Santa Maria, 97105-900 Santa Maria-RS, Brazil

ARTICLE INFO

Article history:
Received 24 June 2011
Accepted 7 October 2011
Available online 17 October 2011

Keywords:
Triazenes
Bifurcated hydrogen interactions
Trifurcated hydrogen interactions

ABSTRACT

The new ligand 1,3-bis(3-methoxy-4-methylbenzoate) triazene (**1**, bmmbt), and the already known ligand 1,3-bis(4-acetylphenyl)triazene (bapht), yield the two new palladium(II) complexes [(bmmbt)Pd(PPh$_3$)$_2$Cl]·DMSO (**2**) and [(bapht)Pd(PPh$_3$)$_2$Cl] (**3**) (Ph = phenyl; DMSO = dimethylsulfoxide). Compound **1** shows the existence of more than one interaction promoting the coupling between the triazene chains. Other remarkable types of interactions in **1** are bifurcated hydrogen contacts and non-classical CH···π bonding. Complexes **2** and **3** present a planar geometry, supported also through bifurcated intramolecular Cl···H–C interactions, as well as the occurrence of trifurcated Cl···H–C *intermolecular* interactions.

1. Introduction

The chemistry of the triazenes (R–N=N–NH–R) started formally in 1859 with the synthesis of 1,3-bis(phenyl)triazene by Griess [1]. Nevertheless, only during the decade of 60 this type of molecules has received attention with biological and technological purposes. At that time Shealy and co-workers reported the synthesis of 5-(3,3-dimethyl-1-triazenes) imidazole-4-carboxamide, clinically known as Dacarbazine [2–4]. Dacarbazine® is currently prescribed as a chemotherapeutic for the treatment of metastatic malignant melanoma, brain tumors, leukemia and Hodgkin's disease [5].

Taking advantage of the recognized ability of triazenes regarding the alkylation of DNA, Rachid et al. [6] have attained a single molecule presenting multiple antiproliferative action, based upon a synergistic mechanism which gives greater efficiency to the synthesized compound. The remarkable species was able to interact with the receptor of epidermal cellular growth factor, being also able to connect simultaneously to DNA, inhibiting or impairing their functions. This molecule inhibited both the growth and proliferation of tumors after decomposition at physiological pH. Fig. 1 represents the possible hydrolytic pathway for the triazene-containing molecule.

Besides this confirmed biological applicability, triazenes seem also to act as facilitators of arenes coupling to silicon surfaces, with major applications in the semiconductors chemistry and nano electronics [7]. Recently, Gothelf and Ferapontovo [8] have reported the use of triazenes also for immobilization and characterization of oligonucleotides.

Acting as ligands, the triazene units [–N–N=N–] exhibit high versatility regarding coordination modes, as a result of its geometry and the presence of electron donor sites. The ligands can act as monodentate, bidentate, chelate or bridge-forming, showing a remarkable ability to suit the stereochemical requirements to perform a wide variety of transition metal complexes [9–12], as shown in Fig. 2.

There are only few reports in the literature about the existence of palladium complexes containing triazene fragments. In one of these, Bombieri et al. [13] describe a possible mechanism involving reactions between triazene ligands and Pd(II), showing the existence of a pentacoordinated intermediate complex in which the triazene ligand achieves a four-membered ring chelate with the metal, according to Fig. 3 [13]. This mechanism involves a fluxional arrangement in solution, i.e., the Pd–N η^1 bond migrates in relation to the nitrogen atoms of the diazoaminic chain.

It has been already reported that triazenes show a noteworthy trend to achieve intermolecular, secondary metal–ligand and ligand–ligand interactions due to hydrogen bonding. Such characteristics make these species also proficient to assemble unique supramolecular aggregates. Recently some examples of these classes of compounds were discussed, with 1D [14–17] and 2D [18–20] polymeric, supramolecular assemblies. This work deals mainly with the synthesis and the structural characterization of the new symmetrical triazene ligand 1,3-bis(3-methoxy-4-methylbenzoate) triazene (**1**, bmmbt), the already known ligand 1,

---

* Corresponding authors. Tel.: +55 55 3220 8757; fax: +55 55 3220 8031.
E-mail addresses: horner@smail.ufsm.br (M. Hörner), manzonideo@smail.ufsm.br (G. Manzoni de Oliveira).

doi:10.1016/j.poly.2011.10.009

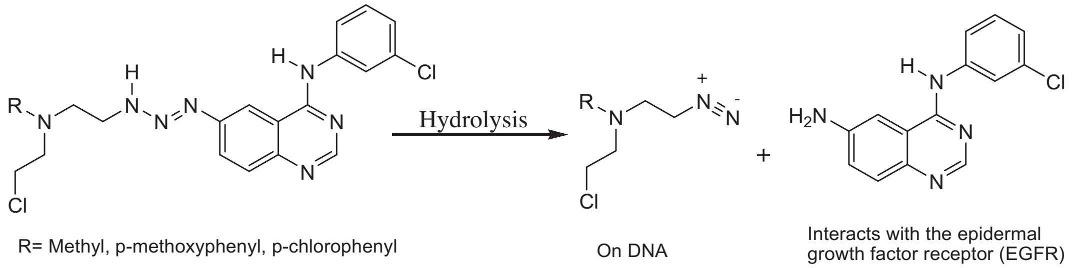

Fig. 1. Possible mechanism of hydrolysis for the triazene-containing molecule.

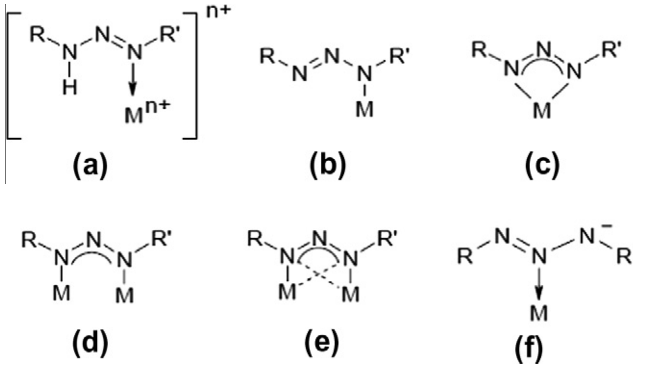

Fig. 2. Main coordination modes of triazenes: (a) neutral monodentate terminal; (b) anionic monodentate terminal; (c) chelating bidentate; (d) bridge-forming; (e) bridge-type syn–syn – η^1:η^1:μ_2; (f) central nitrogen coordination.

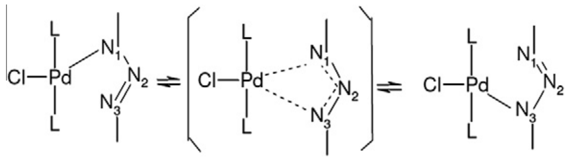

Fig. 3. Mechanism for fluxional monocatenaded triazenes.

3-bis(4-acetylphenyl)triazene (bapht), and the two new palladium(II) complexes [(bmmbt)Pd(PPh_3)$_2$Cl]·DMSO (**2**) and [(bapht)Pd(PPh_3)$_2$Cl] (**3**) (Ph = phenyl; DMSO = dimethylsulfoxide).

With basis on the results here discussed, our aim is also to show the possibilities of obtaining novel and significant hydrogen interactions in the solid state.

2. Experimental

*2.1. Preparation of the ligand 1,3-bis(3-methoxy-4-methylbenzoate) triazene (**1**)*

Ethyl 4-aminobenzoate (0.5 g, 2.76 mmol) was dissolved in a mixture of 15 mL of CH_3COOH and 5 mL of distilled water and the system was cooled to 0 °C. Under constant stirring, sodium nitrite[1] (0.10 g, 2.76 mmol) was also added. After 30 min stirring the medium was neutralized to pH around 6, with a solution of sodium acetate. The yellow precipitate was filtered under vacuum and washed several times with cold water. The product was dried in vacuum. Yield: 53%.

Properties: dark yellow powder. Melting point: 182 °C. *Anal.* Calc. for $C_{18}H_{19}N_3O$ (373.36): C, 57.90; H, 5.09; N, 11.26; O, 25.73. Found: C, 57.60; H, 5.23; N, 11.45; O, 26.71%. IR (KBr) free ligand [cm^{-1}]: 3365 [ν_s, medium (N–H)], 1701 [ν_s, strong (C=O)], 1614 [ν, strong (C–C$_{aryl}$)], 1464 [δ_{as}, medium (CH_3)], 1435 [δ_s, medium (CH_3)], 1284 [ν_s, medium (N–N=N), 1404 [ν, medium (N=N)], 1245 [δ_{as}, medium (C–O–C)], 1031 [δ_s, medium (C–O–C)].

*2.2. Preparation of the complex [(bmmbt)Pd(PPh$_3$)$_2$Cl]·DMSO (**2**)*

0.037 g (0.1 mmol) of **1** was dissolved in methanol by heating the mixture at 65 °C for 30 min. To this solution, 0.070 g (0.1 mmol) of [(PPh_3)$_2$$PdCl_2$] {bis(triphenylphosphine)palladium(II) dichloride} and 0.15 ml of triethylamine were added. After 1 h stirring the color turned intensely dark. After drying, the product was redissolved in DMSO at 50° C. From this solution, tabular orange crystals, suitable for X-ray diffraction, were formed after 3 days. Yield: 35% (based on [(PPh_3)$_2$$PdCl_2$]).

Properties: air stable, tabular, orange crystals. Melting point: 231–233 °C (decomposition). *Anal.* Calc. for $C_{56}H_{54}N_3O_7P_2SClPd$ (1116.87): C, 62.24; H, 4.06; N, 4.6; O, 9.2. Found: C, 62.1; H, 6.03; N, 4.51; O, 9.12%. IR (KBr) complex (cm^{-1}): The N–H band is absent. 1716 [ν_s, s (C=O)], 1594 [ν, s (C–C$_{aryl}$)], 1481 [δ_{as}, m (CH_3)], 1434 [δ_s, m (CH_3)], 1288 [ν_s, m (N–N=N), 1404 [ν, medium (N=N)], 1230 [δ_{as}, m (C–O–C)], 1029 [δ_s, m (C–O–C)], 1125, 692 [ν_s, s, m (P–C$_{aryl}$)].

2.3. Preparation of the ligand 1,3-bis(4-acetylphenyl)triazene

This ligand was prepared according to the modified procedure described by Polanc and co-workers [21]. 4-Amino acetophenone (0.271 g, 2 mmol) was added to a solution of $Na_3Co(NO_2)_6$ (sodium hexanitrocobaltate (III), 0.670 g, 1.87 mmol), in 10 mL of water. The mixture was stirred at room temperature for 4 h, the solid material was isolated by filtration and washed with cold water (3 × 10 mL). Yield: 97%. *Properties:* Melting point: 181–184 °C. *Anal.* Calc.: C, 68.34; H, 5:33; N, 14.94; O, 11.38. Found: C, 68.4; H, 5.39; N, 15.4; O, 11.6%. IR (KBr) free ligand (cm^{-1}): 3197 [ν_s, m (N–H)], 1672 [ν_s, s (C=O)], 1599 [ν, s (C–C$_{aryl}$)], 1440 [δ_s, m (CH_3)], 1398 [ν, m (N=N)], 1270 [ν_s, m (N–N=N)].

*2.4. Preparation of the complex [(bapht)Pd(PPh$_3$)$_2$Cl] (**3**)*

1,3-Bis(4-acetylphenyl)triazene (0.034 g, 0.12 mmol) was dissolved in methanol by heating the mixture at 65 °C for 10 min. Thereafter [(PPh_3)$_2$$PdCl_2$] (0.070 g, 0.1 mmol) and 0.05 ml of triethylamine were added. After 1 h stirring the solution color turned intensely orange. After drying in vacuum, the product was redissolved in pyridine at 50 °C, giving tabular orange crystals, suitable for X-ray diffractometry analysis. Yield: 68% (based on [(PPh_3)$_2$$PdCl_2$]).

Properties: air stable, tabular, orange crystals. Melting point: 228 °C (decomposition at 232 °C). *Anal.* Calc. for $C_{52}H_{44}ClN_3O_2P_2Pd$ (946.69): C, 65.9; H, 4.65; N, 4.44; O, 3.38. Found: C, 66.06; H, 4.5;

---

[1] The procedure carried out with isoamyl nitrite gives a yield of 43%.

Table 1
Crystal data and structure refinement for **1**, **2** and **3**.

	1	**2**	**3**
Empirical formula	$C_{18}H_{19}N_3O$	$C_{56}H_{54}N_3O_7P_2SClPd$	$C_{52}H_{44}ClN_3O_2P_2Pd$
Formula weight	373.36	1116.87	946.69
T (K)	293(2)	293(2)	293(2)
Radiation, λ (Å)	Mo Kα, 0.7107	Mo Kα, 0.7107	Mo Kα, 0.7107
Crystal system	monoclinic	triclinic	monoclinic
Space group	$P2_1/\mathbf{c}$	$P\bar{1}$	$P2_1/\mathbf{c}$
Unit cell dimensions			
a (Å)	12.6400(10)	9.2123(10)	13.2634(3)
b (Å)	14.7190(10)	13.8922(15)	24.2208(6)
c (Å)	9.81900(10)	21.114(2)	14.2368(3)
α (°)	90	79.955(7)	90
β (°)	97.5680(10)	88.328(6)	106.5450(10)
γ (°)	90	86.048(6)	90
V (Å^3)	1810.89(3)	2654.0(5)	4384.21(17)
Z	4	2	4
Calculated density (g cm^{-3})	1.369	1.398	1.434
Absorption coefficient (mm^{-1})	0.104	0.554	0.603
F(000)	784	1152	1944
Crystal size (mm)	0.312 × 0.11 × 0.074	0.160 × 0.103 × 0.087	0.799 × 0.372 × 0.290
θ (°)	1.63–23.57	1.49–26.84	1.81–28.33
Index ranges	$-15 \leq h \leq 15$, $-18 \leq k \leq 18$, $-12 \leq l \leq 12$	$-11 \leq h \leq 11$, $-17 \leq k \leq 16$, $-26 \leq l \leq 26$	$-17 \leq h \leq 17$, $-32 \leq k \leq 32$, $-19 \leq l \leq 14$
Reflections collected	15635	22782	76303
Reflections unique	3861 [R_{int} = 0.0378]	10532 [R_{int} = 0.0630]	10887 [R_{int} = 0.0322]
Completeness to theta maximum (%)	99.8	98.2	99.6
Absorption correction	GAUSSIAN	GAUSSIAN	GAUSSIAN
Maximum and minimum transmission	0.9987 and 0.9383	0.99895 and 0.9136	0.9987and 0.9209
Refinement method	full-matrix least-squares on F^2	full-matrix least-squares on F^2	full-matrix least-squares on F^2
Data/restraints/parameters	3861/0/245	10532/0/649	10887/9/550
Goodness-of-fit (GOF) on F^2	1.02	0.970	1.053
Final R indices [$I > 2\sigma(I)$]	R_1 = 0.0463, wR_2 = 0.1189	R_1 = 0.0531, wR_2 = 0.1108	R_1 = 0.0296, wR_2 = 0.0725
R indices (all data)	R_1 = 0.0864, wR_2 = 0.1499	R_1 = 0.0979, wR_2 = 0.1329	R_1 = 0.0377, wR_2 = 0.0785
Largest difference peak and hole (e Å^{-3})	0.263 and −0.174	1.379 and −1.085	1.424 and −0.716

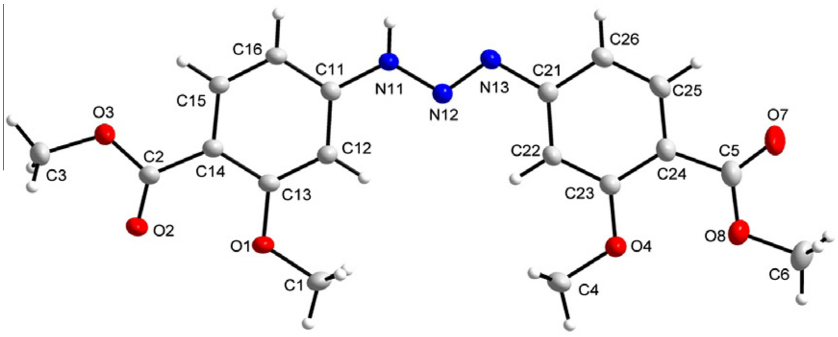

Fig. 4. Molecular structure of the ligand 1,3-bis(3-methoxy-4-methylbenzoate) triazene (**1**). The thermal ellipsoids are represented in a percentage of 30%.

Table 2
Bond lengths (Å) and angles (°) of selected triazene compounds described in the literature.

	Bond lengths (Å)		Bond angles (°)		
	N1–N2	N2═N3	C_{aryl} –N1–N2	N1–N2–N3	N2–N3–C_{aryl}
[23]	1.316(5)	1.285(3)	117.70(2)	112.78(2)	113.79(2)
[24]	1.335(4)	1.271(3)	119.03(3)	112.93(2)	111.87(3)
[25]	1.332(7)	1.267(7)	120.20(5)	111.60(5)	112.90(5)

N, 4.40; O, 3.8%. IR (KBr) complex (cm^{-1}): The N–H band is absent. 1733 [ν_s, s (C═O)], 1673 [ν, s (C–C_{aryl})], 1480 [δ_{as}, m (CH_3)], 1435 [δ_s, m (CH_3)], 1265 [ν_s, m (N–N═N)], 1390 [δ_{as}, m (N═N)], 1146, 693 [ν_s, s, m (P–C_{aryl})].

2.5. X-ray structural determination

Data were collected with a Bruker APEX II CCD area-detector diffractometer and graphite-monochromatized Mo Kα radiation. The structures were solved by direct methods using SHELXS-97 [22]. Subsequent Fourier-difference map analyses yielded the positions of the non-hydrogen atoms. Refinements were carried out with the SHELXL-97 package [22]. All refinements were made by full-matrix least-squares on F^2 with anisotropic displacement parameters for all non-hydrogen atoms. Hydrogen atoms were included in the refinement in calculated positions. Crystal data and more details of the data collections and refinements are contained in Table 1.

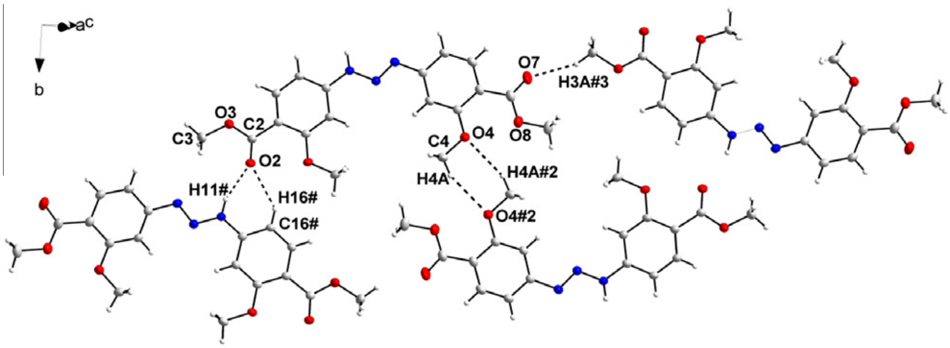

Fig. 5. Representation of the O···H secondary interactions for the free triazene ligand **1** along the crystallographic *bc* plane.

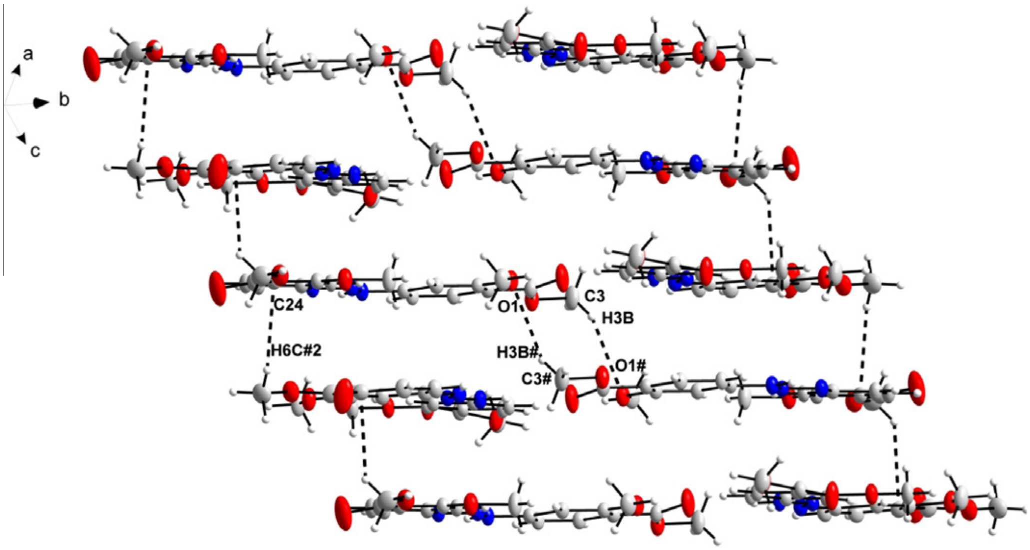

Fig. 6. Representation of the hydrogen interactions (dashed lines) between the layers of crystallization in **1**.

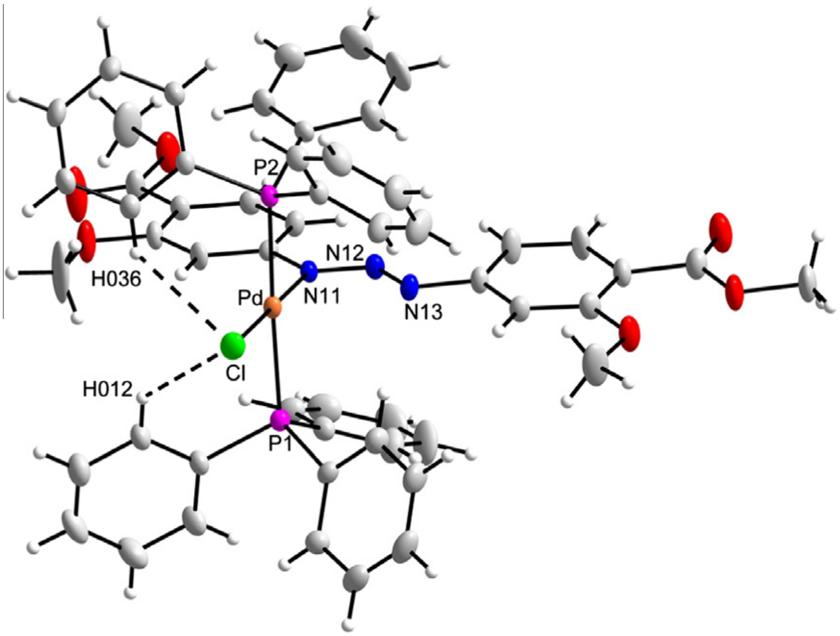

Fig. 7. Molecular structure of [(bmmbt)Pd(PPh$_3$)$_2$Cl]·DMSO (**2**). The thermal ellipsoids are represented in a percentage of 30%. The dashed lines show a bifurcated Cl···H interaction. For clarity, the DMSO molecule does not appear.

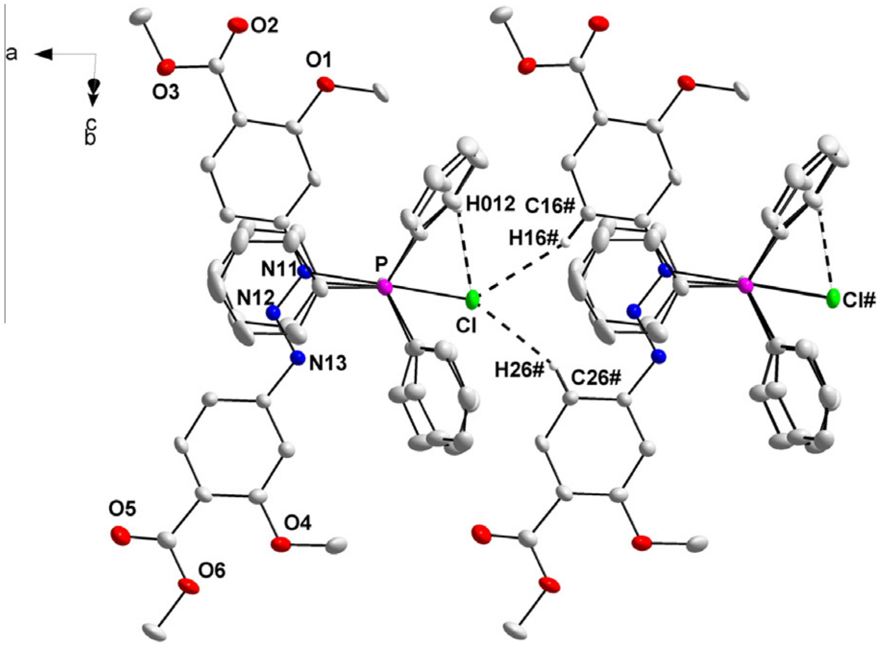

Fig. 8. Representation of [(bmmbt)Pd(PPh$_3$)$_2$Cl]·DMSO (**2**) showing the intra- and intermolecular trifurcated acceptor Cl···H–C interactions of the palladium complex (**2**). For clarity the hydrogen atoms are not shown.

3. Results and discussion

3.1. Crystal structure

The molecular structure of a single triazene ligand **1** is represented in Fig. 4. The bond distance N12–N11 (1.335(2) Å) of **1** is smaller than the characteristic value for a N–N single bond (1.44 Å), while the distance N13–N12 (1.264(2) Å) is larger than the typical N═N double bond distance (1.24 Å). The distances and angles involving the bonds N11–C11 and N13–C21 {N11–C11 = 1.384(3) Å; N12–N11–C11 = 120.83(16)°}/{C21–N13 = 1.416(3) Å; N12–N13–C21 = 112.89(17)°} are shorter than those expected for a single N–C$_{aryl}$ bond (1.452 Å for secondary amines, NHR$_2$). Thus, all the bonds previously cited indicate partial double bond character, implying a delocalization of π electrons in the triazenido chains. Table 2 shows some values of bond lengths and angles for selected reported triazene compounds.

Fig. 5 depicts the reachable (secondary) interactions between the molecules of the free ligand **1** nearby the crystallographic *bc* plane. There is a predominance of bifurcated hydrogen interactions [26–29] between (N11)H11···O2 and (C16)H16#···O2 with distances of 2.093(2) and 2.485(2) Å respectively, and classical

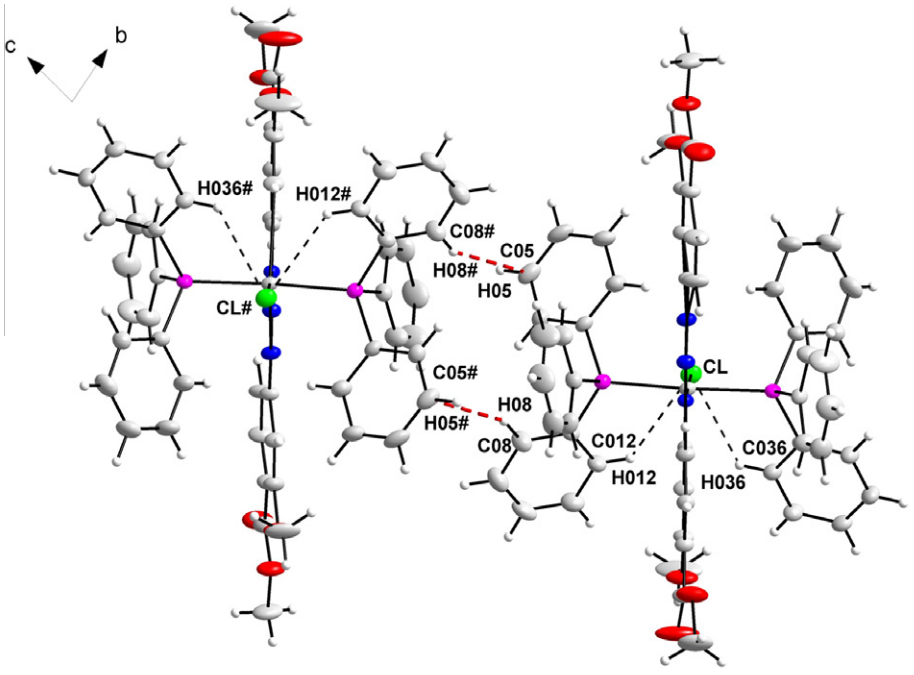

Fig. 9. Representation of complex **2** along the crystallographic *bc* plane, showing the secondary, bifurcated and non-classical (C···H) hydrogen interactions.

interactions between the atoms (C5)O7$\cdots$H3$_A$#3 in the order of 2.392(2) Å. Moreover, is also evident the formation of rings by the reciprocal coupling of the methoxy groups O4$\cdots$H4$_A$#2(C4#2) and (C4)H4$_A\cdots$O4#2 with a distance of 2.626(2) Å (symmetry transformations used to generate equivalent atoms: (#) $1-x$, $0.5+y$, $0.5-z$; (#2) $2-x$, $1-y$, $2-z$; (#3) $-1+x$, $0.5-y$, $-1.5+z$).

Besides the existence of the mentioned interactions, according to Fig. 6 it seems to be evident that there is more than one type of secondary contact promoting the coupling between the triazenido layers. An interesting pairing is achieved by the reciprocal interaction between the groups (C3#)H3$_B$#$\cdots$O1 and (C3)H3$_B\cdots$O1#, with a distance of 2.701(2) Å. Another remarkable type of interaction in the synthesized molecule is the hydrogen non-classical CH$\cdots\pi$ contact. For these weak interactions is assigned a distance of 2.822(2) Å between the atoms (C6)H6$_C\cdots$C24#2(aryl) (symmetry transformations used to generate equivalent atoms: (#) $1-x$, $1-y$, $-z$; (#2) x, $0.5-y$, $0.5+z$).

The CH$\cdots\pi$ interaction has attracted considerable interest due to its importance for several parameters, such as the control of the crystalline packing [30], the structural organization of biological molecules [31] and some processes of molecular recognition [32]. Despite the importance of the CH$\cdots\pi$ interactions, the physical nature of this process is yet not clear, since the precise evaluation of the energy involved in the interaction is difficult to quantify. In view of this, the CH$\cdots\pi$ interaction has been treated as a hydrogen bond. Nevertheless, in contrast with the conventional hydrogen bonds, the directionality of the CH$\cdots\pi$ interaction is also very poor. In this regard, statistical analysis of crystal structures also show that CH$\cdots\pi$ interactions prefer to point toward the aromatic ring, being, however, not perpendicular to the π plane of the ring. According to quantum mechanical calculations, the energy associated with this interaction is approximately 1.5–2.5 kcal mol^{-1} [33–35].

In the structure of complex [(bmmbt)Pd(PPh$_3$)$_2$Cl]·DMSO (**2**), displayed in Fig. 7, the triazene ligand coordinates to Pd(II) in a monodentade way. The formal negative charge of the triazenido chain, as well as the charge of the Cl$^-$ ligand, are counter balanced by the central cation Pd^{2+}, so that the neutrality of the complex is achieved. The coordination polyhedron of the metal atom is consistent with the examples in the literature, since the interaction N13$\cdots$Pd is not strong enough to produce a distorted square geometry. Undoubtedly, the bifurcated intramolecular Cl$\cdots$H–C interactions H012 and H036 must be emphasized, since they also support the complex structure and the geometry of the metal atom. The distances of the bifurcated interaction are 2.814(3) and 2.795(6) Å respectively, and the H012$\cdots$Cl$\cdots$H036 angle is 64.53(3)°.

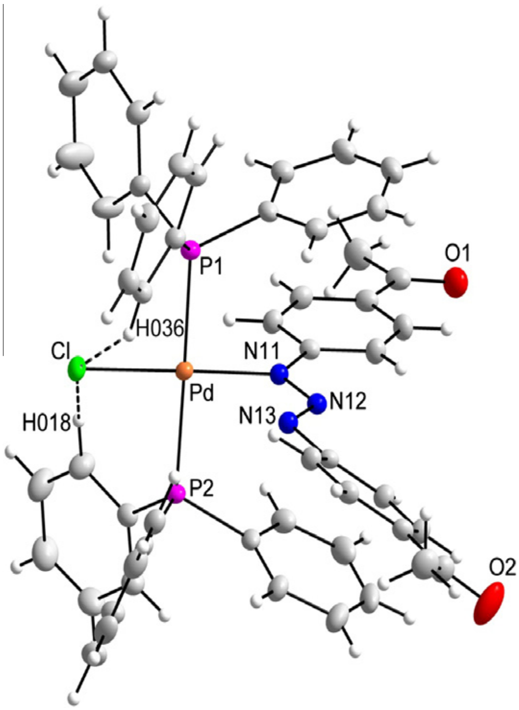

Fig. 10. Molecular structure of [(bapht)Pd(PPh$_3$)$_2$Cl] (**3**). The thermal ellipsoids are represented in a percentage of 50%.

The representation of complex **2** along the *ab* plane, depicted in Fig. 8, allows the visualization of a further bifurcated *intermolecular* Cl$\cdots$H–C interaction, between the atoms (C16#)H16#$\cdots$Cl (2.786(7)) and (C26#)H26#$\cdots$Cl (2.671(8) Å). The H16#$\cdots$Cl$\cdots$H26# angle has 70.08(3)°, and these intermolecular bonds support the growth of the polymeric supramolecular assembly of complex **2** (see Fig. 8, symmetry transformations used to generate equivalent atoms: (#) $-1x$, y, z). If we consider only these three secondary

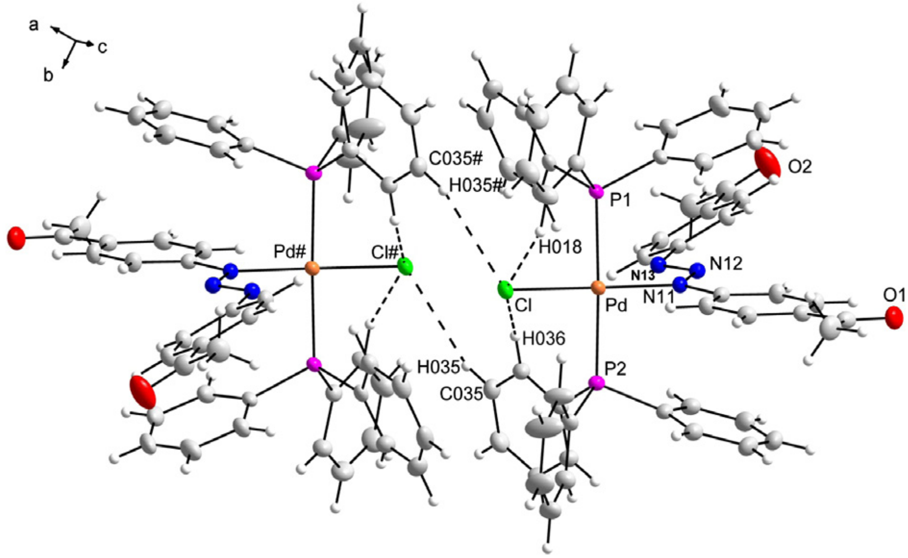

Fig. 11. Centrosymmetric dimer and trifurcated hydrogen interactions formed by the association of two neighboring molecules of [(bapht)Pd(PPh$_3$)$_2$Cl] (**3**). The thermal ellipsoids are represented in a percentage of 50%.

Cl···H–C interactions appearing in Fig. 8, we are talking about *trifurcated acceptor* Cl···H–C bonds.

Fig. 9 shows two neighboring molecules of complex **2** along the *bc* plane. As is clear to see in this position, there are two bifurcated intramolecular Cl···H–C interactions and a intermolecular, centrosymmetric pair of non-classical hydrogen bonds, between the atoms H08/C05# and H08#/C05, with a distance of 2.806 Å (symmetry code (#): $1 - x, -y, 2 - z$). Each of these units can be viewed as a dimer related by an inversion center, and its linkage through further $H08^{x}\cdots C05^{y}$ "double" interactions produces a 1-D supramolecular arrangement (see Fig. 9).

Fig. 10 displays the molecular structure of the second title complex, $[(bapht)Pd(PPh_3)_2Cl]$ (3), which is structurally similar to the previous described complex **2**. The coordination model is the same, with the triazenido ligand coordinating in a monodentate way the divalent cation Pd(II). Also in **3** the neutrality of the complex is achieved through the coordination of a chloride ligand to the metal ion. A bifurcated intramolecular interaction between the hydrogen atoms of the near located aromatic rings and the chloride ligand are also present (H036 and H018), however, in this case, the Cl···H–C distances are slightly shorter than in **2** (2.730(2) and 2.679(1) Å respectively), although the H···Cl···H angle appears significantly altered (154.42(1)°).

Fig. 11 shows the interesting association of two molecules of **3**, in a similar manner to that already seen for **2** (see Fig. 9). The linkage of the neighboring molecules of **3** occurs, however, under formation of a third secondary, intermolecular H···Cl interaction, i.e., attaining a trifurcated hydrogen bonding. A good explanation for the increase of the bond angle between the atoms of hydrogen and chloride in the bifurcated H···Cl interaction in **3** is this type of intermolecular trifurcated donation, involving three *receivers* [36–39]. This interaction is also responsible for the achievement of a centrosymmetric dimer (Fig. 11), but, unlike complex **2**, the dimers of complex **3** do not interact with each other, preventing the formation of supramolecular assemblies in the crystal lattice. The distances between the atoms involved in the trifurcated interactions in the dimers of complex **3** are 2.679(1), 2.730(2) and 2.875(1) Å for H018···Cl, H036···Cl and H035#···Cl, respectively. The bond angles are 68.15(2)° (H035#···Cl···H018) and 120.3(1)° (H035#···Cl···H036) (symmetry transformations used to generate equivalent atoms: (#) $2 - x, 1 - y, 1 - z$).

4. Conclusions

The synthesis of organic ligands containing diazoaminic fragments and their further deprotonation and coordination to a metal center such as palladium revealed itself a new and efficient alternative for the obtention of crystalline solids with potential supramolecular trends, besides numerous forked hydrogen interactions. Supramolecular structures containing these interactions allow the full development of the crystal engineering, thus enabling the understanding of peculiar features of these new materials. Since the main scope of this work is related with the secondary hydrogen bonds, we have quoted the separation between hydrogen and the acceptor atoms, instead of the separation between the donor (mostly C) and acceptor atoms. Given the uncertainty associated with the location of the H atoms using X-ray crystallography, we have not fixed the hydrogens (as commonly done), but evaluated its charge densities with measurement times significantly longer than usual. With this procedure we have attained more accurate hydrogen bonds distances.

After these first reported results, a next step would be the modification of the steric and electronic effects of the suitable ligands, probably also including phosphines. The triazenes used in this work were of great importance to seek preliminary evidences, thus, enabling us to select the best data for the search of new, specific interactions.

Acknowledgment

Fapergs – Fundação de Amparo à Pesquisa do Estado do Rio Grande do Sul. Edital N^{o} 003/2009.

Appendix A. Supplementary data

CCDC 818520, 818521 and 818522 contains the supplementary crystallographic data for **1**, **2** and **3**. These data can be obtained free of charge via http://www.ccdc.cam.ac.uk/conts/retrieving.html, or from the Cambridge Crystallographic Data Centre, 12 Union Road, Cambridge CB2 1EZ, UK; fax: (+44) 1223-336-033; or e-mail: deposit@ccdc.cam.ac.uk.

References

[1] P. Griess, Proc. Roy. Soc. London 9 (1859) 594.
[2] F.A. Schid, D.J. Hutchinson, Cancer Res. 7 (1974) 1671.
[3] Y.F. Shealy, C.A. Krauth, J.A. Montgomery, J. Org. Chem. 27 (1962) 2150.
[4] H. Druckrey, S. Ivankovic, R. Preussmann, Naturwissenschaften 54 (1967) 171.
[5] M. Sanada, Y. Takagi, R. Ito, M. Sekiguchi, DNA Repair 3 (2004) 413.
[6] Z. Rachid, F. Brahimi, Q. Qiu, C. Williams, J.M. Hartley, J.A. Hartley, B.J. Jean-Claude, J. Med. Chem. 50 (2007) 2605.
[7] D.M. Khramov, C.W. Bielawski, J. Org. Chem. 72 (2007) 9407.
[8] M.N. Hansen, E. Farjami, M. Kristiansen, L. Clima, S.U. Pedersen, K. Daasbjerg, E.E. Ferapontova, K.V. Gothelf, J. Org. Chem. 75 (8) (2010) 2474.
[9] D.S. Moore, S.D. Robinson, Adv. Inorg. Chem. Radiochem. 30 (1986) 1.
[10] M. Hörner, G. Manzoni de Oliveira, J.S. Oliveira, W.M. Teles, C.A.L. Filgueiras, J. Beck, J. Organomet. Chem. 691 (2006) 251.
[11] J. T Lenan, H.A. Roman, A.R. Barrow, J. Chem. Soc., Dalton Trans. (1992) 2183.
[12] A.S. Peregudov, D.N. Kravtso, G.I. Drogunova, Z.A. Starikova, A.I. Yanovsky, J. Organomet. Chem. 597 (2000) 164.
[13] G. Bombieri, A. Immirzi, L. Toniolo, Inorg. Chem. 15 (10) (1976) 2428.
[14] M. Hörner, G. Manzoni de Oliveira, J.S. Bonini, H. Fenner, J. Organomet. Chem. 691 (2006) 655.
[15] M. Hörner, G. Manzoni de Oliveira, J.A. Naue, J. Daniels, J. Beck, J. Organomet. Chem. 691 (2006) 1051.
[16] M. Hörner, G. Manzoni de Oliveira, M.B. Behm, H. Fenner, Z. Anorg. Allg. Chem. 632 (2006) 615.
[17] M. Hörner, G. Manzoni de Oliveira, L.C. Visentin, R.S. Cezar, Inorg. Chim. Acta 359 (2006) 4667.
[18] M. Hörner, G. Manzoni de Oliveira, V.F. Giglio, L.C. Visentin, F. Broch, J. Beck, Inorg. Chim. Acta 359 (2006) 2309.
[19] M. Hörner, G. Manzoni de Oliveira, L. Bresolin, A.B. de Oliveira, Inorg. Chim. Acta 359 (2006) 4631.
[20] M. Hörner, G. Manzoni de Oliveira, E.G. Koehler, L.C. Visentin, J. Organomet. Chem. 691 (2006) 1311.
[21] B. Stefane, M. Kotevar, S. Polanc, J. Org. Chem. 62 (1997) 7165.
[22] G.M. Sheldrick, Acta Crystallogr., Sect. A 64 (2008) 112.
[23] J.T. Leman, J. Braddck-Wilking, A.J. Coolong, A.R. Barron, Inorg. Chem. 32 (1993) 4324.
[24] R. Anulewicz, Acta Crystallogr., Sect. C 53 (1997) 345.
[25] M. Hörner, I.C. Casagrande, J. Bordinhão, C.M. Mössmer, Acta Crystallogr., Sect. C 58 (2002) o193.
[26] L. Checinska, S.J. Grabowski, M. Malecka, J. Phys. Org. Chem. 16 (2003) 213.
[27] LaTeca S. Glass, B. Nguyen, K.D. Goodwin, C. Dardonville, W.D. Wilson, E.C. Long, M.M. Georgiadis, Biochemistry 48 (2009) 5943.
[28] P. Sharma, M. Chawla, S. Sharma, A. Mitra, RNA 16 (2010) 942.
[29] G.R. Desiraju, T. Steiner, The Weak Hydrogen Bond – In Structural Chemistry and Biology (International Union of Crystallography – Monographs on Crystallography), Oxford University Press, 2001.
[30] K. Saigo, Y. Kobayashi, Chem. Rec. 7 (2007) 47.
[31] V. Spiwok, P. Lipovová, T. Skálová, E. Buchtelová, J. Hasek, B. Králová, Carbohydr. Res. 339 (2004) 2275.
[32] P.S. Lakshminarayanan, D.K. Kumar, P. Ghosh, J. Am. Chem. Soc. 128 (2006) 9600.
[33] T.J. Mooibroek, P. Gamez, J. Reedijk, Cryst. Eng. Comm. 10 (2008) 1501.
[34] I. Caracelli, J. Zukerman-Schpector, S.H. Maganhi, H.A. Stefani, R. Guadagnin, E.R.T. Tiekink, J. Braz. Chem. Soc. 21/11 (2010) 2155.
[35] M.A.P. Martins, D.N. Moreira, C.P. Frizzo, P.T. Campos, K. Longhi, M.R.B. Marzari, N. Zanatta, H.G. Bonacorso, J. Mol. Struct. 969 (2010) 111.
[36] D. Ghoshal, A.K. Ghosh, J. Ribas, G. Mostafa, N.R. Chaudhuri, Cryst. Eng. Comm. 7 (2005) 616.
[37] T. Steiner, Angew. Chem., Int. Ed. 41 (2002) 48.
[38] G.R. Desiraju, S.K. Panigrahi, Proteins Struct. Funct. Bioinform. 67 (2007) 128.
[39] R.G. Gonnade, M.M. Bhadbhade, M.S. Shashidhar, Chem. Commun. 22 (2004) 2530.